Alzheimer's & Dementia: Diagnosis, Assessment & Disease Monitoring 10 (2018) 638-646

Neuroimaging

Multimodal neuroimaging study of cerebrovascular disease, amyloid deposition, and neurodegeneration in Alzheimer's disease progression

Patrick J. Lao*, Adam M. Brickman, for the Alzheimer's Disease Neuroimaging Initiative[1]

Taub Institute for Research on Alzheimer's Disease and the Aging Brain, College of Physicians and Surgeons, Columbia University, New York, NY, USA

Abstract

Introduction: Cerebrovascular disease (CVD) is not currently considered a core pathological feature of Alzheimer's disease (AD), but mounting evidence suggests that concurrent CVD may exacerbate AD progression. The purpose of this study was first to examine the relationship among amyloid, CVD, and neurodegeneration and second to examine the extent to which amyloid and CVD pathology drive subsequent neurodegeneration over time.

Methods: Six hundred eight (224 normal controls, 291 mild cognitive impairment, 93 AD) subjects from the Alzheimer's Disease Neuroimaging Initiative with longitudinal AV45 positron emission tomography imaging and MR imaging were investigated.

Results: Amyloid and white matter hyperintensity (WMH) burden increased across clinical diagnosis groups (normal control < mild cognitive impairment < AD). Amyloid pathology and WMH volume were related to lower cortical thickness, while WMH burden was associated with neurodegenerative/atrophic changes over time in key AD-related brain regions.

Discussion: CVD and AD may be etiologically independent, but our findings suggest that CVD should be considered explicitly for its effect on AD progression.

Keywords: Alzheimer's disease; Cerebrovascular disease; Neurodegeneration; Amyloid PET; White matter hyperintensity; Alzheimer's Disease Neuroimaging Initiative

1. Introduction

Current pathogenic models of Alzheimer's disease (AD) propose that the pathophysiological process begins with amyloid-β plaque accumulation, represented as a sigmoid curve with a slow, age-related accumulation followed by a rapid, disease-related accumulation and finally ending in saturation [1–5]. Approximately 20%–40% of adults aged over 60 years demonstrate elevated levels of amyloid, despite being cognitively normal [1], suggesting that while amyloid might be necessary for disease pathogenesis, it is not sufficient to explain the clinical symptoms and course of AD. After the initial amyloid deposition, or even concurrent with amyloid deposition, there is regionally specific deposition of neurofibrillary tangles made up of hyperphosphorylated tau protein [1]. Further downstream, structural magnetic resonance imaging (MRI) has shown that cortical atrophy mirrors the distribution of tau pathology and is a ubiquitous feature of clinical AD [6,7]. Cortical thinning as measured on structural MRI is a biomarker for neuronal death and is the most proximal biomarker to cognitive decline [1].

Clinical diagnosis of AD during an individual's lifetime may differ from pathological diagnosis of AD at postmortem analysis, and a meta-analysis showed there is relatively poor agreement between clinical and pathological diagnoses of

The authors have declared that no conflict of interest exists.

[1]Data used in preparation of this article were obtained from the Alzheimer's Disease Neuroimaging Initiative (ADNI) database (adni.loni.usc.edu). As such, the investigators within the ADNI contributed to the design and implementation of ADNI and/or provided data but did not participate in analysis or writing of this report. A complete listing of ADNI investigators can be found at http://adni.loni.usc.edu/wp-content/uploads/how_to_apply/ADNI_Acknowledgement_List.pdf.

*Corresponding author. Tel.: +1 212-342-1399; Fax: +1 212-342-1838.
E-mail address: pjl2133@cumc.columbia.edu

https://doi.org/10.1016/j.dadm.2018.08.007

AD, with sensitivity and specificity ranging between 71%–87% and 44%–71%, respectively [8,9]. The inclusion of AD biomarkers has been suggested as a method for increasing the accuracy of clinical diagnoses [10,11]. However, even at a given AD biomarker profile, there is still a large amount of within-individual variability in clinical AD development and progression, which may be attributable to genetic and lifestyle factors, as well as the presence of other critical morbidities [12]. Mixed brain pathologies account for dementia in most older individuals, with 75% of individuals with a pathological AD diagnosis also showing one or more vascular pathologies [12]. Cerebrovascular disease (CVD) is of particular interest because it occurs in approximately 16%–46% of elderly and up to 51% in the oldest old [12].

White matter hyperintensities (WMHs) are areas of increased signal visualized on T2-weighted MRI sequences that result from macrostructural changes that lead to decreased lipid content and increased water content. The most widely accepted biological model of WMH etiology is that damage to blood vessels leads to chronic hypoperfusion [13], while other biological explanations, such as Wallerian degeneration, suggest that primary damage from pathology, such as neurofibrillary tangles, leads to axonal death [14,15]. WMHs are widely used as an imaging-based biomarker of small vessel CVD [16–18]. There is a large pathological overlap between small vessel CVD and AD, and WMH burden has been linked to cortical atrophy, cognitive decline, and clinical AD diagnosis [18,19]. Importantly, there is strong age dependence for both amyloid and WMH burden, and there are common vascular risk factors for AD and CVD [19]. Understanding the interplay between amyloid deposition and CVD, and how they each contribute to neurodegeneration, may provide insight into potentially shared pathways of disease. In the present study, we investigated the longitudinal relationship between biomarkers of amyloid, CVD, and neurodegeneration, and the extent to which early events, such as amyloid or CVD, drive neurodegeneration over time in a large, longitudinal cohort.

2. Methods

Data used in the preparation of this article were obtained from the Alzheimer's Disease Neuroimaging Initiative (ADNI) database (adni.loni.usc.edu). The ADNI was launched in 2003 as a public-private partnership, led by a principal investigator, Michael W. Weiner, MD. The primary goal of ADNI has been to test whether serial MRI, positron emission tomography, other biological markers, and clinical and neuropsychological assessment can be combined to measure the progression of mild cognitive impairment (MCI) and early AD. For up-to-date information, see www.adni-info.org.

Six hundred four subjects (n = 224 normal controls [NCs], 291 MCI, 93 AD) from the ADNI study underwent longitudinal AV45 positron emission tomography imaging, as well as T1, T2, and proton density MRI scans to quantify fibrillar amyloid deposition, WMH, and cortical thickness, respectively. Subjects had up to 12 time points (up to 10 years) of imaging data (N for each visit after visit 1: 216, 215, 189, 168, 157, 135, 112, 63, 27, 15, 3, 1 NC; 267, 261, 253, 240, 215, 175, 127, 73, 38, 18, 7, 1 MCI; 82, 76, 69, 59, 50, 17 AD). Global WMH volume was estimated at University of California-Davis using spatial and contextual priors for WMH as the sum of cortical lobes (frontal, occipital, parietal, temporal) [20–22]. Global AV45 standard uptake value ratio (SUVR) was estimated at University of California-Berkeley as the ratio of cortical regions implicated in Thal staging of amyloid plaques (frontal, anterior/posterior cingulate, lateral parietal, lateral temporal) to a composite white matter reference region (whole cerebellum, brainstem/pons, subcortical white matter) [23,24]. Global cortical thickness was estimated at University of California-San Francisco using FreeSurfer 5.1 (http://surfer.nmr.mgh.harvard.edu/) with longitudinal processing [25] as the mean of AD-associated regions (medial/inferior temporal, temporal pole, angular gyrus, superior/inferior frontal, superior parietal, supramarginal gyrus, precuneus) [26,27].

Analyses of covariance and chi-squared tests compared continuous and categorical demographic information, respectively, across clinical diagnostic group. Similarly, mean AV45 SUVR, WMH volume, and cortical thickness, and rates of change in each, were compared across clinical diagnostic group. Imaging biomarkers were used in two ways: first as categorical variables and second as fully continuous variables. Similar to the method of amyloid positivity determination at University of California-Berkeley [28], thresholds for abnormal amyloid levels were determined as the upper 95% confidence interval of the mean in normal controls. Using all available data from ADNI (i.e., not restricted to the 608 subjects with all three imaging biomarkers), abnormal biomarker threshold was determined for amyloid (n = 833 NC scans, 0.82 SUVR) and log-transformed WMH (n = 1774 NC scans, 0.80 mm^3). Chi-squared tests were used to compare the prevalence of biomarker abnormality by diagnosis.

Next, a series of pairwise linear mixed-effects models with unbalanced designs and repeated measures was used to investigate associations between AV45 SUVR, WMH volume, and cortical thickness, including a random subject factor (e.g., AV45 SUVR on cortical thickness, AV45 SUVR on WMH volume, and WMH volume on cortical thickness). Since linear mixed-effects models handle unbalanced designs (e.g., unequal number of subjects or visits with each imaging biomarker) by using all available data, models have different degrees of freedom. Full models including all three biomarkers simultaneously were used to investigate additive or synergistic contributions of amyloid and CVD on neurodegeneration (e.g., AV45 SUVR and WMH volume on cortical thickness). Pairwise and full growth curve models were also run to investigate the associations between

AV45 and/or WMH volume on cortical thinning rate (e.g., AV45 SUVR*time on cortical thickness, WMH volume*-time on cortical thickness).

All models were tested with covariate adjustment by clinical diagnostic group, and statistical significance was evaluated at $P < .05$ (IBM SPSS Statistics for Windows, Version 23.0, IBM Corp., Armonk, NY). Covariates of interest included subject-mean centered age, apolipoprotein epsilon 4 (APOE-ε4), sex, education, and baseline intracranial total volume (ICV). Linear mixed-effects models are presented in tables as follows: Biomarker ~ Clinical Diagnoses + Age + Sex + APOE4 + Education + ICV + Intercept. Growth curve models are as follows: Biomarker ~ Time + Clinical Diagnoses + Age + Sex + APOE4 + Education + ICV + Time*Clinical Diagnoses + Time*Age + Time*Sex + Time*APOE4 + Time*Education + Time*ICV + Intercept, but are presented only as Time interaction parameters in subsequent tables.

3. Results

Diagnostic groups differed in the frequency of APOE-ε4 (APOE4+: NC: 26% < MCI: 46% < AD: 74%; $\chi(3) = 63.6$, $P < .001$), sex distribution (male: NC: 46% < MCI: 59% NC < AD: 56%; $\chi(3) = 8.6$, $P = .04$), number of years of education (NC: 17 ± 3 years > MCI: 16 ± 3, NC > AD: 16 ± 3; $F(2,603) = 3.8$, $P = .02$), and ICV (NC: 1508 ± 156 cm^3 <MCI: 1550 ± 157, AD: 1505 ± 161 <MCI; $F(2,553) = 5.9$, $P = .003$), but not by baseline age (NC: 74 ± 6 years, MCI: 73 ± 7 years, AD: 73 ± 8; $F(2,603) = 1.6$, $P = .21$). As expected, AV45 SUVR increased (NC < MCI < AD), WMH volume increased (NC < AD), and cortical thickness decreased (NC > MCI > AD) across diagnostic groups (Table 1). AV45 SUVR rate decreased across diagnostic groups (NC > MCI, NC > AD), indicating a possible plateau in amyloid deposition during MCI or AD (Table 1), proposed in the sigmoid trajectories of biomarker progression [1,2]. Rate of change in WMH volume and cortical thinning rate were not significantly different between clinical diagnostic groups (Table 1). While not significant, rate of change in WMH volume increased across clinical diagnostic groups as expected, but cortical thinning rate in AD was slower than that in the normal control or MCI group (Table 1).

Following the amyloid cascade hypothesis, downstream neurodegeneration in key AD regions would not be likely to occur without sufficient amyloid burden. To investigate the apparent slowing in cortical thinning rate in AD, individuals were categorized by biomarker abnormality rather than clinical diagnosis (Fig. 1). The proportion of individuals with abnormally high amyloid increased across diagnostic groups, in the expected direction (NC: 30.1% < MCI: 53.4% < AD: 84.2%; $\chi(2) = 139.6$, $P < .001$). Similarly, abnormally high WMH volume prevalence increased across diagnostic groups as expected (NC: 55.5% < MCI: 60.9% < AD: 80.3%; $\chi(2) = 71.1$, $P < .001$). Note that there

Table 1
AV45 standard uptake value ratio (SUVR), white matter hyperintensity (WMH) volume, and cortical thickness and rates of change in each by clinical diagnosis

Outcome	WMH volume	WMH volume rate	Amyloid SUVR	Amyloid SUVR rate	Cortical thickness	Cortical thinning rate
Intercept	B = 0.08 [−8.9, 9.1] $P = .95$	B = −2.8 [−8.7, 3.10] $P = .38$	**B = 1.00 [0.83, 1.16] $P < .001$**	B = −0.011 [−0.045, 0.022] $P = .26$	**B = 2.44 [2.27, 2.62] $P < .001$**	B = −0.088 [−0.197, 0.021] $P = .15$
Clinical diagnosis	B_{AD} = 1.10 [0.09, 2.12] B_{MCI} = 0.83 [−0.01, 1.67] $P = .098$	B_{AD} = 0.32 [−0.37, 1.01] B_{MCI} = 0.51 [−0.10, 1.12] $P = .16$	**B_{AD} = 0.053 [0.032, 0.074] B_{MCI} = 0.027 [0.012, 0.042] $P < .001$**	B_{AD} = −0.006 [−0.013, 0.0004] B_{MCI} = −0.001 [−0.006, 0.005] $P = .11$	**B_{AD} = −0.099 [−0.121, −0.077] B_{MCI} = −0.025 [−0.042, −0.007] $P < .001$**	B_{AD} = 0.009 [−0.004, 0.022] B_{MCI} = 0.006 [−0.005, 0.017] $P = .79$
Age	**B = 0.52 [0.39, 0.66] $P < .001$**	**B = 0.075 [0.006, 0.143] $P = .034$**	**B = 0.004 [0.002, 0.007] $P = .001$**	B = −1.6E-5 [−0.0009, 0.0009] $P = .97$	**B = −0.015 [−0.018, −0.013] $P < .001$**	**B = −0.001 [−0.002, −2.4E-5] $P = .045$**
Sex	B_M = −0.13 [−1.88, 1.62] $P = .88$	B_M = −0.14 [−1.31, 1.03] $P = .81$	B_M = −0.02 [−0.056, 0.007] $P = .12$	B_M = −0.0002 [−0.006, 0.006] $P = .96$	B_M = −0.031 [−0.065, 0.003] $P = .074$	B_M = −0.0005 [−0.024, 0.023] $P = .97$
APOE4	B_{E4} = 1.07 [−0.37, 2.52] $P = .15$	B_{E4} = 0.09 [−0.89, 1.08] $P = .85$	**B_{E4} = 0.144 [0.120, 0.169] $P < .001$**	**B_{E4} = 0.008 [0.003, 0.014] $P = .002$**	**B_{E4} = −0.034 [−0.063, −0.006] $P = .018$**	B_{E4} = −0.014 [−0.035, 0.006] $P = .17$
Education	B = −0.06 [−0.32, 0.20] $P = .66$	B = −0.02 [−0.20, 0.15] $P = .80$	**B = −0.005 [−0.010, −0.0004] $P = .035$**	B = −6.5E-5 [−0.001, 0.0009] $P = .89$	B = 0.003 [−0.002, 0.008] $P = .31$	B = 0.001 [−0.003, 0.005] $P = .64$
Intracranial total volume	B = 4.0E-6 [−1.1E-6, 9.1 E-6] $P = .13$	B = 1.6E-6 [−1.7E-6, 4.9 E-6] $P = .33$	B = 1.3E-8 [−8.3E-8, 1.1 E-7] $P = .79$	B = 6.7E-9 [−1.1E-8, 2.5 E-8] $P = .46$	B = 2.3E-8 [−7.6E-8, 1.2 E-7] $P = .65$	B = 2.1E-8 [−3.7E-8, 7.9 E-8] $P = .47$

NOTE. Values are presented as mean parameter estimate [95% CI] and bolded if $P < .05$. Rows represent all the variables included in a single linear mixed effects or growth curve model (column).

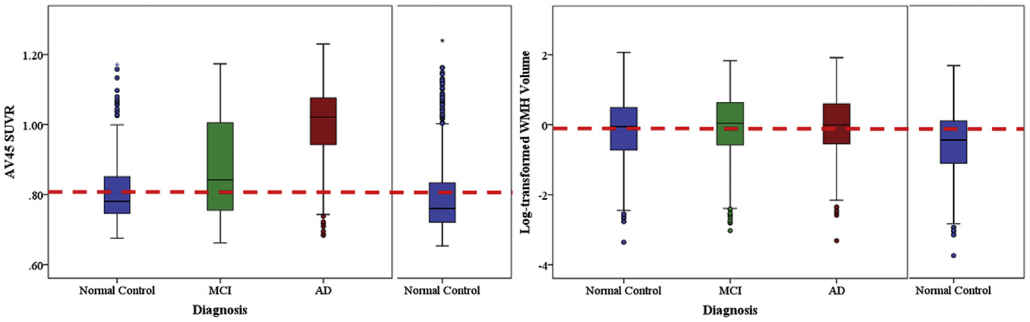

Fig. 1. Distribution of AV45 standard uptake value ratio (SUVR) and log-transformed white matter hyperintensity (WMH) volume by clinical diagnostic group. Dotted line represents abnormality threshold (upper 95% confidence interval in normal control group from larger sample [right]) for each biomarker. * Represents outliers in SPSS graphs. Abbreviations: AD, Alzheimer's disease; MCI, mild cognitive impairment.

was an incomplete prevalence (e.g., <100%) of abnormally high amyloid in the clinically diagnosed AD group and that the subjects with the highest WMH volume were in the NC group (Fig. 1). Cortical thickness was significantly lower in individuals with abnormally high amyloid compared to normally low amyloid (Table 2). Cortical thinning rate was only significantly different from zero in individuals with abnormally high WMH volume, but not significantly different between the four biomarker abnormality classifications (Table 2).

To further investigate the associations among amyloid, WMH, and neurodegeneration, imaging biomarkers were used as fully continuous variables in independent, pairwise linear mixed-effects models (Fig. 2). AV45 SUVR was not associated with WMH volume (Supplementary Table 1). AV45 SUVR was negatively associated with cortical thickness and was significantly different between clinical diagnostic groups such that the association was more negative in MCI and AD compared with NC (Supplementary Table 2). Similarly, WMH volume was negatively associated with cortical thickness and was significantly different between clinical diagnostic groups such that the association was more negative in MCI and AD compared with NC (Supplementary Table 2). In a full linear mixed-effects model (i.e., including all three imaging biomarkers), the same associations survive as in the pairwise models (Table 3).

Moreover, independent, pairwise growth curve models, which include time interactions (Fig. 2), showed that baseline AV45 SUVR was not associated with rate of change in WMH, but higher baseline WMH volume was associated with faster AV45 SUVR rate (Supplementary Table 1). There was no significant association between baseline AV45 SUVR and cortical thinning rate (Supplementary Table 2). There was a significant interaction between clinical diagnosis and baseline WMH volume on cortical thinning rate such that there was more cortical thinning with higher WMH volume in MCI and AD compared to NC (Supplementary Table 2). In a full growth curve model, cortical thinning rate was not significantly associated with baseline WMH or baseline AV45 SUVR (Table 3). There were no significant interactions between AV45 SUVR and WMH volume on cortical thickness in the full linear mixed-effects model or on cortical thinning rate in the full growth curve model.

4. Discussion

Profiles of multiple, abnormal biomarkers provide more insight into variations in the AD pathophysiological process compared with single biomarkers or clinical diagnosis, especially in the context of concurrent small vessel CVD, which we operationally define as WMH burden. This multimodal

Table 2
Cortical thickness and cortical thinning rate by biomarker abnormality classifications

	Cortical thickness	Cortical thinning rate
Biomarker abnormality profile	$B_{LOW\ Amyloid,\ LOW\ WMH}$ = 2.73 [2.58, 2.88]	$B_{LOW\ Amyloid,\ LOW\ WMH}$ = −0.002 [−0.016, 0.013]
	$B_{LOW\ Amyloid,\ HIGH\ WMH}$ = 2.61 [2.58, 2.64]	**$B_{LOW\ Amyloid,\ HIGH\ WMH}$ = −0.008 [−0.012, −0.003]****
	$B_{HIGH\ Amyloid,\ LOW\ WMH}$ = 2.47 [2.38, 2.57]*	$B_{HIGH\ Amyloid,\ LOW\ WMH}$ = −0.002 [−0.011, 0.008]
	$B_{HIGH\ Amyloid,\ HIGH\ WMH}$ = 2.51 [2.49, 2.54]*	**$B_{HIGH\ Amyloid,\ HIGH\ WMH}$ = −0.008 [−0.012, −0.005]****
Age	**B = −0.028 [−0.036, −0.019] *P* < .001**	B = 8.1E-5 [−0.003, 0.003] *P* = .96
Sex	B_M = −0.016 [−0.065, 0.034] *P* = .53	B_M = 0.007 [−0.014, 0.029] *P* = .50
APOE4	B_{E4+} = −0.009 [−0.054, 0.037] *P* = .70	B_{E4+} = −0.011 [−0.032, 0.009] *P* = .27
Education	B = 0.008 [−0.0003, 0.015] *P* = .059	**B = 0.004 [0.0003, 0.007] *P* = .03**
Intracranial total volume	B = 8.1E-8 [−7.8E-8, 2.4E-7] *P* = .32	B = 1.3E-8 [-5.5E-8, 8.1E−8] *P* = .71

* Denotes significant difference from reference group (low amyloid, low WMH). ** Denotes significant difference from 0.

NOTE. Values are presented as mean parameter estimate [95% CI] and bolded if *P* < .05. Rows represent all the variables included in a single linear mixed effects or growth curve model (column).

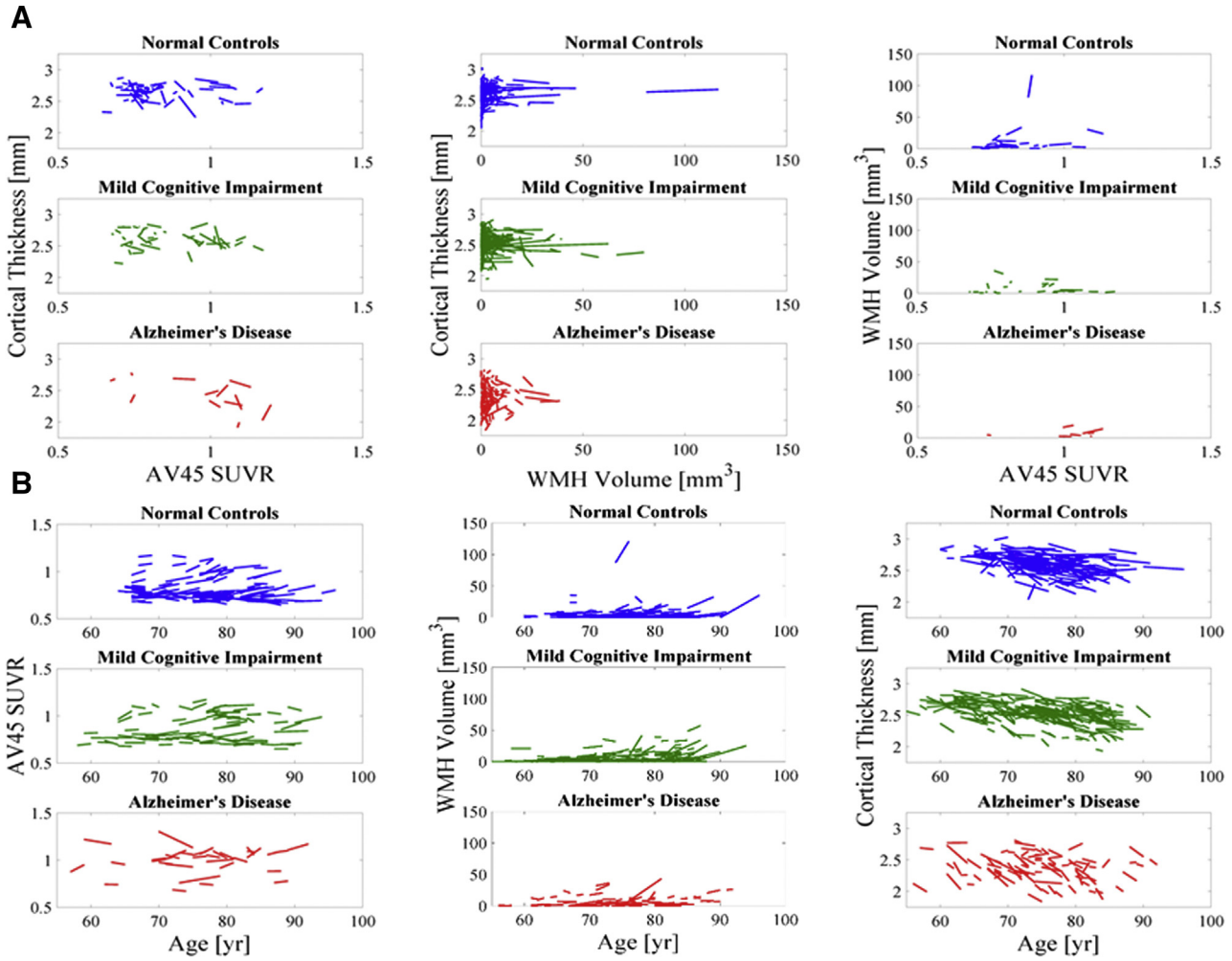

Fig. 2. (A) Pairwise spaghetti plots between longitudinal measures of cortical thickness, AV45 standard uptake value ratio (SUVR), and log-transformed white matter hyperintensity (WMH) volume. Each line represents a subject. (B) Spaghetti plots between longitudinal measures of cortical thickness, AV45 SUVR, and log-transformed WMH volume against time.

neuroimaging study indicates that increased amyloid pathology and WMH volume are related to lower cortical thickness and, importantly, suggests that WMHs are associated with neurodegeneration over time in key AD-associated regions, even in the absence of substantial amyloid burden. Similar to our findings, some studies suggest an additive effect of amyloid and CVD on neurodegeneration [12,29,30], but others have suggested that CVD might act synergistically with AD pathology [31–34].

There was an expected overlap of small vessel CVD and AD pathophysiology in that there was an increase in amyloid burden and WMH volume, as well as a decrease in cortical thickness across clinical diagnostic groups. While the finding was not significant, there was an unexpected slowing of cortical thinning rate in clinically defined AD compared with NC and MCI. Using biomarker classifications rather than clinical diagnostic groups, the focus of our analysis was shifted toward AD-associated and small vessel CVD–associated pathophysiology over clinical symptomatology. While we did not use a particularly sophisticated method to estimate abnormal amyloid or WMH burden thresholds, our thresholds produced similar results to previous studies [28]. Thirty percent of normal controls had abnormally high amyloid burden, consistent with approximately 20%–40% of elderly individuals demonstrating elevated levels of amyloid, despite being cognitively normal [1]. In addition, we found that 15% of clinically diagnosed AD cases had normally low amyloid, similar to the frequency of AD cases without pathology at autopsy [9]. It should be noted that inclusion criteria of ADNI included a score of less than 4 on the Hachinski scale for history of hypertension and stroke, effectively including subjects with a low-to-moderate vascular risk [16]. Individuals with the highest WMH volume were normal controls, possibly reflecting that symptomatic individuals (e.g., MCI, AD) with high degrees of CVD were excluded because of concerns of "mixed" pathology. Consequently, the WMH volumes in ADNI (0.08–1.18 cm^3) are smaller than those observed in

Table 3
Full linear mixed-effects models and growth curve models between AV45 standard uptake value ratio (SUVR), white matter hyperintensity (WMH) volume, and cortical thickness by clinical diagnosis

	Cortical thickness		Cortical thinning rate		
Intercept	B = 2.73 [2.41, 3.05] $P < .001$	B = 2.72 [2.36, 3.07] $P < .001$	B = −0.053 [−0.198, 0.092] $P = .39$	B = −0.048 [−0.209, 0.113] $P = .21$	
Clinical diagnosis	B_{AD} = 0.38 [0.08, 0.68]	B_{AD} = 0.43 [0.03, 0.83]	B_{AD} = −0.009 [−0.149, 0.132]	B_{AD} = −0.072 [−0.283, 0.140]	
	B_{MCI} = 0.18 [−0.06, 0.41] $P = .048$	B_{MCI} = 0.17 [−0.14, 0.47] $P = .103$	B_{MCI} = −0.005 [−0.138, 0.128] $P = .99$	B_{MCI} = −0.072 [−0.243, 0.103] $P = .66$	
WMH volume	B = 3.3E-5 [−0.002, 0.002] $P = .30$	B = 0.002 [−0.025, 0.030] $P = .83$	B = 0.0004 [−0.0006, 0.001] $P = .21$	B = −0.002 [−0.014, 0.009] $P = .30$	
WMH volume *	**B_{AD} = 0.001 [−0.003, 0.006]**	B_{AD} = −0.011 [−0.068, 0.045]	B_{AD} = 0.002 [−0.0007, 0.005]	B_{AD} = 0.012 [−0.013, 0.038]	
Clinical diagnosis	**B_{MCI} = −0.004 [−0.008, −0.0004] $P = .044$**	B_{MCI} = −0.003 [−0.038, 0.033] $P = .93$	B_{MCI} = −0.0008 [−0.003, 0.001] $P = .14$	B_{MCI} = 0.010 [−0.009, 0.030] $P = .43$	
Amyloid SUVR	**B = −0.20 [−0.43, 0.04] $P < .001$**	**B = −0.18 [−0.47, 0.10] $P < .001$**	B = −0.026 [−0.142, 0.090] $P = .34$	B = −0.043 [−0.182, 0.095] $P = .93$	
Amyloid SUVR *	**B_{AD} = −0.61 [−0.94, −0.28]**	**B_{AD} = −0.67 [−1.09, −0.25]**	B_{AD} = −0.029 [−0.193, 0.135]	B_{AD} = 0.042 [−0.199, 0.283]	
Clinical diagnosis	**B_{MCI} = −0.23 [−0.50, 0.05] $P = .001$**	**B_{MCI} = −0.21 [−0.57, 0.14] $P = .007$**	B_{MCI} = −0.003 [−0.161, 0.154] $P = .93$	B_{MCI} = 0.074 [−0.132, 0.282] $P = .77$	
WMH volume *		B = −0.003 [−0.034, 0.028]		B = 0.003 [−0.010, 0.017] $P = .37$	
Amyloid SUVR		F(1,343) = 0.005, $P = .95$			
WMH volume *		B_{AD} = 0.012 [−0.04, 0.07]		B_{AD} = −0.011 [−0.039, 0.016]	
Amyloid SUVR * Clinical diagnosis		B_{MCI} = −0.002 [−0.04, 0.04] $P = .88$		B_{MCI} = −0.013 [−0.036, 0.010] $P = .44$	
Age	**B = −0.012 [−0.021, −0.003] $P = .013$**	**B = −0.012 [−0.021, −0.003] $P = .013$**	B = −0.0005 [−0.004, 0.003] $P = .81$	B = −0.0004 [−0.004, 0.004] $P = .84$	
Sex	B_M = −0.014 [−0.056, 0.029] $P = .53$	B_M = −0.014 [−0.056, 0.029] $P = .53$	B_M = −0.011 [−0.030, 0.009] $P = .27$	B_M = −0.011 [−0.030, 0.009] $P = .29$	
APOE4	**B_{E4} = 0.040 [0.0001, 0.079] $P = .049$**	B_{E4} = 0.039 [−0.0001, 0.079] $P = .051$	B_{E4} = 0.007 [−0.012, 0.026] $P = .50$	B_{E4} = 0.006 [−0.014, 0.025] $P = .55$	
Education	B = 0.0006 [−0.006, 0.007] $P = .85$	B = 0.0005 [−0.006, 0.007] $P = .87$	B = 0.002 [−0.0008, 0.005] $P = .15$	B = 0.002 [−0.0008, 0.005] $P = .15$	
Intracranial total volume	B = 5.3E-8 [−8.0E-8, 1.9E-7] $P = .43$	B = 5.6E-8 [−7.7E-8, 1.9E-7] $P = .41$	B = 3.5E−8 [−2.4E-8, 9.4E-8] $P = .25$	B = 4.1E-8 [−2.0E-8, 1.0E-7] $P = .19$	

NOTE. Values are presented as mean parameter estimate [95% CI] and bolded if $P < .05$. Rows represent all the variables included in a single linear mixed effects or growth curve model (column).

other studies (2.5–20.2 cm^3) [35]. These issues may have introduced bias into our analyses, potentially inflating type II statistical error rates (i.e., toward the null hypothesis). Using our abnormality threshold for WMH volume, approximately 55% of NC had high WMH burden at a mean age of approximately 75 years, similar to previous findings [12].

Amyloid burden has been widely shown to be associated with neurodegeneration [36–38], as our results demonstrated. Results are mixed concerning an association between AD pathology and WMH volume [13,18,39,40]. Some studies attribute increased WMH in the context of clinical AD to Wallerian degeneration, or secondary damage due to primary AD pathology [14,15]. Our results demonstrated no direct association between amyloid and WMH volume and that WMH was associated with future decrease in cortical thickness, suggesting that WMHs are not simply a reflection of Wallerian damage but rather promote neurodegeneration. Moreover, we found that baseline WMH volume was associated with amyloid accumulation rate but that baseline amyloid was not associated with WMH volume rate, also suggesting that WMHs are not simply a consequence of amyloidosis and that WMH may drive faster amyloid accumulation. Previous work in the ADNI cohort demonstrated an association between vascular risk factors and WMH volume after adjustment for amyloid burden [16]. Our analyses here found a more negative association between WMH volume and cortical thickness and cortical thinning rate in a composite AD signature region, similar to associations between WMH volume and cortical volume found in the entorhinal cortex [41] or hippocampus [42]. We also found that cortical thinning over time was only significantly different from zero with high WMH burden, regardless of amyloid burden, suggesting that WMHs can indeed promote neurodegenerative changes. Similarly, animal studies demonstrate cortical atrophy in models of impaired cerebrovascular function [43,44], and a previous study showed atrophy in AD-associated regions in the context of CVD but in the absence of AD pathology [45]. Further work is necessary to fully understand the mechanism by which CVD leads to neurodegeneration.

Limitations of the present study include an unbalanced design in which models had different degrees of freedom based on available data, selection bias against overt CVD in the clinically diagnosed MCI and AD groups, and the restriction of biomarker measures to global or AD signature averages. It is possible that WMH volume reflects other pathologies than small vessel CVD, but previous work has shown an association between WMH volume and vascular risk factors in the ADNI cohort [16]. Corrections for multiple comparisons to lower type I error were not performed despite running pairwise and full linear mixed-effects models and growth curve models due to the sampling bias against overt CVD, which would effectively raise the type II error. Strengths of the study include the large, multisite,

multimodal and longitudinal nature of the ADNI study, which allowed us to observe associations even with the bias against overt CVD. A causal relationship between amyloid and WMH burden on cortical thickness cannot be determined definitively in observational studies, but the longitudinal design supports some degree of inference about the temporal ordering of these image-based biomarker changes (i.e., cortical thinning in those with high WMH burden). Future work includes extending this work to voxelwise analyses for more spatially specific conclusions in a population with a higher prevalence of CVD.

Overall, our findings indicate that amyloid burden and WMH volume additively contribute to overall cortical thickness and suggest that WMH volume contributes to the rate of cortical thinning in AD-associated regions, even in the absence of amyloid pathophysiology. In addition, in the presence of substantial amyloid burden, WMH could provide a second hit, increasing the cortical atrophy rate and contributing to clinical symptomatology [29,32]. The respective importance of AD pathophysiology and CVD on neurodegeneration is of crucial significance for the development of effective preventive and therapeutic strategies.

Acknowledgments

Authors' contributions: Study concept and design were performed by Lao and Brickman. Analysis and interpretation of data were performed by Lao and Brickman. Drafting of the article was done by Lao and Brickman. Critical revision of the manuscript for important intellectual content was performed by Lao and Brickman. Statistical analysis was conducted by Lao and Brickman. Administrative, technical, and material support was provided by Lao and Brickman.

Data collection and sharing for this project were funded by the Alzheimer's Disease Neuroimaging Initiative (ADNI) (National Institutes of Health grant U01 AG024904) and DOD ADNI (Department of Defense award number W81XWH-12-2-0012). ADNI is funded by the National Institute on Aging, the National Institute of Biomedical Imaging and Bioengineering, and through generous contributions from the following: AbbVie; Alzheimer's Association; Alzheimer's Drug Discovery Foundation; Araclon Biotech; BioClinica, Inc.; Biogen; Bristol-Myers Squibb Company; CereSpir, Inc.; Cogstate; Eisai Inc.; Elan Pharmaceuticals, Inc.; Eli Lilly and Company; EuroImmun; F. Hoffmann La Roche Ltd and its affiliated company Genentech, Inc.; Fujirebio; GE Healthcare; IXICO Ltd.; Janssen Alzheimer Immunotherapy Research & Development, LLC.; Johnson & Johnson Pharmaceutical Research & Development LLC.; Lumosity; Lundbeck; Merck & Co., Inc.; Meso Scale Diagnostics, LLC.; NeuroRx Research; Neurotrack Technologies; Novartis Pharmaceuticals Corporation; Pfizer Inc.; Piramal Imaging; Servier; Takeda Pharmaceutical Company; and Transition Therapeutics. The Canadian Institutes of Health Research is providing funds to support ADNI clinical sites in Canada. Private sector contributions are facilitated by the Foundation for the National Institutes of Health (www.fnih.org). The grantee organization is the Northern California Institute for Research and Education, and the study is coordinated by the Alzheimer's Therapeutic Research Institute at the University of Southern California. ADNI data are disseminated by the Laboratory for Neuro Imaging at the University of Southern California.

Data used in preparation of this article were obtained from the Alzheimer's Disease Neuroimaging Initiative (ADNI) database (adni.loni.ucla.edu). As such, the investigators within the ADNI contributed to the design and implementation of ADNI and/or provided data but did not participate in the analysis or writing of this article.

Supplementary data

Supplementary data related to this article can be found at https://doi.org/10.1016/j.dadm.2018.08.007.

RESEARCH IN CONTEXT

1. Systematic review: The authors performed a literature search for amyloid deposition, white matter hyperintensity volume, and cortical thickness. While there were published articles that analyzed these metrics in the context of Alzheimer's disease, there were few studies that analyzed all three of these image-based biomarkers simultaneously in a large, longitudinal study.
2. Interpretation: Our findings demonstrate the combined contribution of vascular disease and amyloid deposition to neurodegeneration during Alzheimer's disease progression.
3. Future directions: This article identifies a relationship between vascular disease and Alzheimer's pathophysiology in a large, multisite, longitudinal study. This relationship will be further investigated in an ethnically and racially diverse cohort in which there is a higher risk of vascular disease.

References

[1] Jack CR Jr, Knopman DS, Jagust WJ, Shaw LM, Aisen PS, Weiner MW, et al. Hypothetical model of dynamic biomarkers of the Alzheimer's pathological cascade. Lancet Neurol 2010;9:119–28.

[2] Jack CR Jr, Knopman DS, Jagust WJ, Petersen RC, Weiner MW, Aisen PS, et al. Tracking pathophysiological processes in Alzheimer's disease: an updated hypothetical model of dynamic biomarkers. Lancet Neurol 2013;12:207–16.

[3] Khachaturian ZS. Diagnosis of Alzheimer's disease. Arch Neurol 1985;42:1097–105.
[4] Selkoe DJ. The molecular pathology of Alzheimer's disease. Neuron 1991;6:487–98.
[5] Villemagne VL, Burnham S, Bourgeat P, Brown B, Ellis KA, Salvado O, et al. Amyloid β deposition, neurodegeneration, and cognitive decline in sporadic Alzheimer's disease: a prospective cohort study. Lancet Neurol 2013;12:357–67.
[6] Jack CR Jr, Shiung MM, Gunter JL, O'Brien PC, Weigand SD, Knopman DS, et al. Comparison of different MRI brain atrophy rate measures with clinical disease progression in AD. Neurology 2004; 62:591–600.
[7] Whitwell JL, Przybelski SA, Weigand SD, Knopman DS, Boeve BF, Petersen RC, et al. 3D maps from multiple MRI illustrate changing atrophy patterns as subjects progress from mild cognitive impairment to Alzheimer's disease. Brain 2007;130:1777–86.
[8] Beach TG, Monsell SE, Phillips LE, Kukull W. Accuracy of the clinical diagnosis of Alzheimer disease at National Institute on Aging Alzheimer Disease Centers, 2005-2010. J Neuropathol Exp Neurol 2012; 71:266–73.
[9] Nelson PT, Head E, Schmitt FA, Davis PR, Neltner JH, Jicha GA, et al. Alzheimer's disease is not "brain aging": Neuropathological, genetic, and epidemiological human studies. Acta Neuropathol 2011; 121:571–87.
[10] Dubois B, Feldman HH, Jacova C, Dekosky ST, Barberger-Gateau P, Cummings J, et al. Research criteria for the diagnosis of Alzheimer's disease: revising the NINCDS-ADRDA criteria. Lancet Neurol 2007; 6:734–46.
[11] Sperling RA, Aisen PS, Beckett LA, Bennett DA, Craft S, Fagan AM, et al. Toward defining the preclinical stages of Alzheimer's disease: recommendations from the National Institute on Aging-Alzheimer's Association workgroups on diagnostic guidelines for Alzheimer's disease. Alzheimers Dement 2011;7:280–92.
[12] Kapasi A, DeCarli C, Schneider JA. Impact of multiple pathologies on the threshold for clinically overt dementia. Acta Neuropathol 2017; 134:171–86.
[13] Gurol ME, Irizarry MC, Smith EE, Raju S, Diaz-Arrastia R, Bottiglieri T, et al. Plasma beta-amyloid and white matter lesions in AD, MCI, and cerebral amyloid angiopathy. Neurology 2006;66:23–9.
[14] Coleman M. Axon degeneration mechanisms: Commonality amid diversity. Nat Rev Neurosci 2005;6:889–98.
[15] McAleese KE, Walker L, Graham S, Moya ELJ, Johnson M, Erskine D, et al. Parietal white matter lesions in Alzheimer's disease are associated with cortical neurodegenerative pathology, but not with small vessel disease. Acta Neuropathol 2017;134:459–73.
[16] Scott JA, Braskie MN, Tosun D, Thompson PM, Weiner M, DeCarli C, et al. Cerebral amyloid and hypertension are independently associated with white matter lesions in elderly. Front Aging Neurosci 2015;7:221.
[17] Gunning-Dixon FM, Brickman AM, Cheng JC, Alexopoulos GS. Aging of cerebral white matter: a review of MRI findings. Int J Geriatr Psychiatry 2009;24:109–17.
[18] Thal DR, Attems J, Ewers M. Spreading of amyloid, tau, and microvascular pathology in Alzheimer's disease: Findings from neuropathological and neuroimaging studies. J Alzheimers Dis 2014;42:S421–9.
[19] Brickman AM. Contemplating Alzheimer's disease and the contribution of white matter hyperintensities. Curr Neurol Neurosci Rep 2013;13:415.
[20] Carmichael O, Schwarz C, Drucker D, Fletcher E, Harvey D, Beckett L, et al. Longitudinal changes in white matter disease and cognition in the first year of the Alzheimer disease neuroimaging initiative. Arch Neurol 2010;67:1370–8.
[21] DeCarli C, Fletcher E, Ramey V, Harvey D, Jagust WJ. Anatomical mapping of white matter hyperintensities (WMH): Exploring the relationships between periventricular WMH, deep WMH, and total WMH burden. Stroke 2005;36:50–5.
[22] Yoshita M, Fletcher E, Harvey D, Ortega M, Martinez O, Mungas DM, et al. Extent and distribution of white matter hyperintensities in normal aging, MCI, and AD. Neurology 2006;67:2192–8.
[23] Chen K, Roontiva A, Thiyyagura P, Lee W, Liu X, Ayutyanont N, et al. Improved power for characterizing longitudinal amyloid-beta PET changes and evaluating amyloid-modifying treatments with a cerebral white matter reference region. J Nucl Med 2015;56:560–6.
[24] Landau SM, Fero A, Baker SL, Koeppe R, Mintun M, Chen K, et al. Measurement of longitudinal beta-amyloid change with 18F-florbetapir PET and standardized uptake value ratios. J Nucl Med 2015; 56:567–74.
[25] Reuter M, Schmansky NJ, Rosas HD, Fischl B. Within-subject template estimation for unbiased longitudinal image analysis. Neuroimage 2012;61:1402–18.
[26] Brickman AM, Zahodne LB, Guzman VA, Narkhede A, Meier IB, Griffith EY, et al. Reconsidering harbingers of dementia: Progression of parietal lobe white matter hyperintensities predicts Alzheimer's disease incidence. Neurobiol Aging 2015;36:27–32.
[27] Dickerson BC, Bakkour A, Salat DH, Feczko E, Pacheco J, Greve DN, et al. The cortical signature of Alzheimer's disease: Regionally specific cortical thinning relates to symptom severity in very mild to mild AD dementia and is detectable in asymptomatic amyloid-positive individuals. Cereb Cortex 2009;19:497–510.
[28] Joshi AD, Pontecorvo MJ, Clark CM, Carpenter AP, Jennings DL, Sadowsky CH, et al. Performance characteristics of amyloid PET with florbetapir F 18 in patients with alzheimer's disease and cognitively normal subjects. J Nucl Med 2012;53:378–84.
[29] DeCarli C, Massaro J, Harvey D, Hald J, Tullberg M, Au R, et al. Measures of brain morphology and infarction in the Framingham Heart Study: Establishing what is normal. Neurobiol Aging 2005; 26:491–510.
[30] Vemuri P, Lesnick TG, Przybelski SA, Knopman DS, Preboske GM, Kantarci K, et al. Vascular and amyloid pathologies are independent predictors of cognitive decline in normal elderly. Brain 2015; 138:761–71.
[31] Crystal HA, Schneider JA, Bennett DA, Leurgans S, Levine SR. Associations of cerebrovascular and Alzheimer's disease pathology with brain atrophy. Curr Alzheimer Res 2014;11:309–16.
[32] Provenzano FA, Muraskin J, Tosto G, Narkhede A, Wasserman BT, Griffith EY, et al. White matter hyperintensities and cerebral amyloidosis: necessary and sufficient for clinical expression of Alzheimer disease? JAMA Neurol 2013;70:455–61.
[33] Schneider JA, Wilson RS, Bienias JL, Evans DA, Bennett DA. Cerebral infarctions and the likelihood of dementia from Alzheimer disease pathology. Neurology 2004;62:1148–55.
[34] Rabin JS, Schultz AP, Hedden T, Viswanathan A, Marshall GA, Kilpatrick E, et al. Interactive associations of vascular risk and beta-amyloid burden with cognitive decline in clinically normal elderly individuals: Findings from the Harvard Aging Brain Study. JAMA Neurol 2018;75:1124–31.
[35] Ramirez J, McNeely AA, Scott CJM, Masellis M, Black SE. White matter hyperintensity burden in elderly cohort studies: The Sunnybrook Dementia Study, Alzheimer's Disease Neuroimaging Initiative, and Three-City Study. Alzheimers Dement 2016;12:203–10.
[36] Becker JA, Hedden T, Carmasin J, Maye J, Rentz DM, Putcha D, et al. Amyloid-beta associated cortical thinning in clinically normal elderly. Ann Neurol 2011;69:1032–42.
[37] Dore V, Villemagne VL, Bourgeat P, Fripp J, Acosta O, Chetelat G, et al. Cross-sectional and longitudinal analysis of the relationship between Abeta deposition, cortical thickness, and memory in cognitively unimpaired individuals and in Alzheimer disease. JAMA Neurol 2013; 70:903–11.
[38] Chetelat G, Villemagne VL, Villain N, Jones G, Ellis KA, Ames D, et al. Accelerated cortical atrophy in cognitively normal elderly with high beta-amyloid deposition. Neurology 2012;78:477–84.

[39] Grimmer T, Faust M, Auer F, Alexopoulos P, Forstl H, Henriksen G, et al. White matter hyperintensities predict amyloid increase in Alzheimer's disease. Neurobiol Aging 2012;33:2766–73.

[40] Hedden T, Mormino EC, Amariglio RE, Younger AP, Schultz AP, Becker JA, et al. Cognitive profile of amyloid burden and white matter hyperintensities in cognitively normal older adults. J Neurosci 2012; 32:16233–42.

[41] Guzman VA, Carmichael OT, Schwarz C, Tosto G, Zimmerman ME, Brickman AM, et al. White matter hyperintensities and amyloid are independently associated with entorhinal cortex volume among individuals with mild cognitive impairment. Alzheimers Dement 2013; 9:S124–31.

[42] Rizvi B, Narkhede A, Last BS, Budge M, Tosto G, Manly JJ, et al. The effect of white matter hyperintensities on cognition is mediated by cortical atrophy. Neurobiol Aging 2018;64:25–32.

[43] Gesztelyi G, Finnegan W, DeMaro JA, Wang JY, Chen JL, Fenstermacher J. Parenchymal microvascular systems and cerebral atrophy in spontaneously hypertensive rats. Brain Res 1993;611:249–57.

[44] Tajima A, Hans FJ, Livingstone D, Wei L, Finnegan W, DeMaro J, et al. Smaller local brain volumes and cerebral atrophy in spontaneously hypertensive rats. Hypertension 1993;21:105–11.

[45] Fein G, Di Sclafani V, Tanabe J, Cardenas V, Weiner MW, Jagust WJ, et al. Hippocampal and cortical atrophy predict dementia in subcortical ischemic vascular disease. Neurology 2000;55:1626–35.